Physics Letters B 721 (2013) 212–219

Contents lists available at SciVerse ScienceDirect

Physics Letters B

www.elsevier.com/locate/physletb

Measurement of the combined rapidity and p_T dependence of dijet azimuthal decorrelations in $p\bar{p}$ collisions at $\sqrt{s} = 1.96$ TeV

D0 Collaboration

V.M. Abazov [ag], B. Abbott [bq], B.S. Acharya [aa], M. Adams [au], T. Adams [as], G.D. Alexeev [ag], G. Alkhazov [ak], A. Alton [bf,1], A. Askew [as], S. Atkins [bd], K. Augsten [g], C. Avila [e], F. Badaud [j], L. Bagby [at], B. Baldin [at], D.V. Bandurin [as], S. Banerjee [aa], E. Barberis [be], P. Baringer [bb], J.F. Bartlett [at], U. Bassler [o], V. Bazterra [au], A. Bean [bb], M. Begalli [b], L. Bellantoni [at], S.B. Beri [y], G. Bernardi [n], R. Bernhard [t], I. Bertram [an], M. Besançon [o], R. Beuselinck [ao], P.C. Bhat [at], S. Bhatia [bh], V. Bhatnagar [y], G. Blazey [av], S. Blessing [as], K. Bloom [bi], A. Boehnlein [at], D. Boline [bn], E.E. Boos [ai], G. Borissov [an], A. Brandt [bt], O. Brandt [u], R. Brock [bg], A. Bross [at], D. Brown [n], J. Brown [n], X.B. Bu [at], M. Buehler [at], V. Buescher [v], V. Bunichev [ai], S. Burdin [an,2], C.P. Buszello [am], E. Camacho-Pérez [ad], B.C.K. Casey [at], H. Castilla-Valdez [ad], S. Caughron [bg], S. Chakrabarti [bn], D. Chakraborty [av], K. Chakravarthula [bd], K.M. Chan [az], A. Chandra [bv], E. Chapon [o], G. Chen [bb], S.W. Cho [ac], S. Choi [ac], B. Choudhary [z], S. Cihangir [at], D. Claes [bi], J. Clutter [bb], M. Cooke [at], W.E. Cooper [at], M. Corcoran [bv], F. Couderc [o], M.-C. Cousinou [l], D. Cutts [bs], A. Das [aq], G. Davies [ao], S.J. de Jong [ae,af], E. De La Cruz-Burelo [ad], F. Déliot [o], R. Demina [bm], D. Denisov [at], S.P. Denisov [aj], S. Desai [at], C. Deterre [u,4], K. DeVaughan [bi], H.T. Diehl [at], M. Diesburg [at], P.F. Ding [ap], A. Dominguez [bi], A. Dubey [z], L.V. Dudko [ai], D. Duggan [bj], A. Duperrin [l], S. Dutt [y], A. Dyshkant [av], M. Eads [av], D. Edmunds [bg], J. Ellison [ar], V.D. Elvira [at], Y. Enari [n], H. Evans [ax], V.N. Evdokimov [aj], G. Facini [be], L. Feng [av], T. Ferbel [bm], F. Fiedler [v], F. Filthaut [ae,af], W. Fisher [bg], H.E. Fisk [at], M. Fortner [av], H. Fox [an], S. Fuess [at], A. Garcia-Bellido [bm], J.A. García-González [ad], G.A. García-Guerra [ad,3], V. Gavrilov [ah], W. Geng [l,bg], C.E. Gerber [au], Y. Gershtein [bj], G. Ginther [at,bm], G. Golovanov [ag], P.D. Grannis [bn], S. Greder [p], H. Greenlee [at], G. Grenier [q,r], Ph. Gris [j], J.-F. Grivaz [m], A. Grohsjean [o,4], S. Grünendahl [at], M.W. Grünewald [ab], T. Guillemin [m], G. Gutierrez [at], P. Gutierrez [bq], J. Haley [be], L. Han [d], K. Harder [ap], A. Harel [bm], J.M. Hauptman [ba], J. Hays [ao], T. Head [ap], T. Hebbeker [s], D. Hedin [av], H. Hegab [br], A.P. Heinson [ar], U. Heintz [bs], C. Hensel [u], I. Heredia-De La Cruz [ad], K. Herner [bf], G. Hesketh [ap,6], M.D. Hildreth [az], R. Hirosky [bw], T. Hoang [as], J.D. Hobbs [bn], B. Hoeneisen [i], J. Hogan [bv], M. Hohlfeld [v], I. Howley [bt], Z. Hubacek [g,o], V. Hynek [g], I. Iashvili [bl], Y. Ilchenko [bu], R. Illingworth [at], A.S. Ito [at], S. Jabeen [bs], M. Jaffré [m], A. Jayasinghe [bq], M.S. Jeong [ac], R. Jesik [ao], P. Jiang [d], K. Johns [aq], E. Johnson [bg], M. Johnson [at], A. Jonckheere [at], P. Jonsson [ao], J. Joshi [ar], A.W. Jung [at], A. Juste [al], E. Kajfasz [l], D. Karmanov [ai], P.A. Kasper [at], I. Katsanos [bi], R. Kehoe [bu], S. Kermiche [l], N. Khalatyan [at], A. Khanov [br], A. Kharchilava [bl], Y.N. Kharzheev [ag], I. Kiselevich [ah], J.M. Kohli [y], A.V. Kozelov [aj], J. Kraus [bh], A. Kumar [bl], A. Kupco [h], T. Kurča [q,r], V.A. Kuzmin [ai], S. Lammers [ax], G. Landsberg [bs], P. Lebrun [q,r], H.S. Lee [ac], S.W. Lee [ba], W.M. Lee [as], X. Lei [aq], J. Lellouch [n], D. Li [n], H. Li [bw], L. Li [ar], Q.Z. Li [at], J.K. Lim [ac], D. Lincoln [at], J. Linnemann [bg], V.V. Lipaev [aj], R. Lipton [at], H. Liu [bu], Y. Liu [d], A. Lobodenko [ak], M. Lokajicek [h], R. Lopes de Sa [bn], R. Luna-Garcia [ad,7], A.L. Lyon [at], A.K.A. Maciel [a], R. Magaña-Villalba [ad], S. Malik [bi], V.L. Malyshev [ag], Y. Maravin [bc], J. Martínez-Ortega [ad], R. McCarthy [bn], C.L. McGivern [ap], M.M. Meijer [ae,af], A. Melnitchouk [at], D. Menezes [av], P.G. Mercadante [c], M. Merkin [ai], A. Meyer [s], J. Meyer [u], F. Miconi [p], N.K. Mondal [aa], M. Mulhearn [bw], E. Nagy [l], M. Naimuddin [z], M. Narain [bs], R. Nayyar [aq], H.A. Neal [bf], J.P. Negret [e], P. Neustroev [ak], H.T. Nguyen [bw], T. Nunnemann [w], J. Orduna [bv], N. Osman [l], J. Osta [az], M. Padilla [ar], A. Pal [bt], N. Parashar [ay], V. Parihar [bs], S.K. Park [ac], R. Partridge [bs,5], N. Parua [ax], A. Patwa [bo], B. Penning [at], M. Perfilov [ai], Y. Peters [u], K. Petridis [ap], G. Petrillo [bm], P. Pétroff [m], M.-A. Pleier [bo],

0370-2693/$ – see front matter
http://dx.doi.org/10.1016/j.physletb.2013.03.029

P.L.M. Podesta-Lerma [ad,8], V.M. Podstavkov [at], A.V. Popov [aj], M. Prewitt [bv], D. Price [ax], N. Prokopenko [aj], J. Qian [bf], A. Quadt [u], B. Quinn [bh], M.S. Rangel [a], K. Ranjan [z], P.N. Ratoff [an], I. Razumov [aj], P. Renkel [bu], I. Ripp-Baudot [p], F. Rizatdinova [br], M. Rominsky [at], A. Ross [an], C. Royon [o], P. Rubinov [at], R. Ruchti [az], G. Sajot [k], P. Salcido [av], A. Sánchez-Hernández [ad], M.P. Sanders [w], A.S. Santos [a,9], G. Savage [at], L. Sawyer [bd], T. Scanlon [ao], R.D. Schamberger [bn], Y. Scheglov [ak], H. Schellman [aw], C. Schwanenberger [ap], R. Schwienhorst [bg], J. Sekaric [bb], H. Severini [bq], E. Shabalina [u], V. Shary [o], S. Shaw [bg], A.A. Shchukin [aj], R.K. Shivpuri [z], V. Simak [g], P. Skubic [bq], P. Slattery [bm], D. Smirnov [az], K.J. Smith [bl], G.R. Snow [bi], J. Snow [bp], S. Snyder [bo], S. Söldner-Rembold [ap], L. Sonnenschein [s], K. Soustruznik [f], J. Stark [k], D.A. Stoyanova [aj], M. Strauss [bq], L. Suter [ap], P. Svoisky [bq], M. Titov [o], V.V. Tokmenin [ag], Y.-T. Tsai [bm], D. Tsybychev [bn], B. Tuchming [o], C. Tully [bk], L. Uvarov [ak], S. Uvarov [ak], S. Uzunyan [av], R. Van Kooten [ax], W.M. van Leeuwen [ae], N. Varelas [au], E.W. Varnes [aq], I.A. Vasilyev [aj], P. Verdier [q,r], A.Y. Verkheev [ag], L.S. Vertogradov [ag], M. Verzocchi [at], M. Vesterinen [ap], D. Vilanova [o], P. Vokac [g], H.D. Wahl [as], M.H.L.S. Wang [at], J. Warchol [az], G. Watts [bx], M. Wayne [az], J. Weichert [v], L. Welty-Rieger [aw], A. White [bt], D. Wicke [x], M.R.J. Williams [an], G.W. Wilson [bb], M. Wobisch [bd], D.R. Wood [be], T.R. Wyatt [ap], Y. Xie [at], R. Yamada [at], S. Yang [d], T. Yasuda [at], Y.A. Yatsunenko [ag], W. Ye [bn], Z. Ye [at], H. Yin [at], K. Yip [bo], S.W. Youn [at], J.M. Yu [bf], J. Zennamo [bl], T.G. Zhao [ap], B. Zhou [bf], J. Zhu [bf], M. Zielinski [bm], D. Zieminska [ax], L. Zivkovic [n]

[a] *LAFEX, Centro Brasileiro de Pesquisas Físicas, Rio de Janeiro, Brazil*
[b] *Universidade do Estado do Rio de Janeiro, Rio de Janeiro, Brazil*
[c] *Universidade Federal do ABC, Santo André, Brazil*
[d] *University of Science and Technology of China, Hefei, People's Republic of China*
[e] *Universidad de los Andes, Bogotá, Colombia*
[f] *Charles University, Faculty of Mathematics and Physics, Center for Particle Physics, Prague, Czech Republic*
[g] *Czech Technical University in Prague, Prague, Czech Republic*
[h] *Center for Particle Physics, Institute of Physics, Academy of Sciences of the Czech Republic, Prague, Czech Republic*
[i] *Universidad San Francisco de Quito, Quito, Ecuador*
[j] *LPC, Université Blaise Pascal, CNRS/IN2P3, Clermont, France*
[k] *LPSC, Université Joseph Fourier Grenoble 1, CNRS/IN2P3, Institut National Polytechnique de Grenoble, Grenoble, France*
[l] *CPPM, Aix-Marseille Université, CNRS/IN2P3, Marseille, France*
[m] *LAL, Université Paris-Sud, CNRS/IN2P3, Orsay, France*
[n] *LPNHE, Universités Paris VI and VII, CNRS/IN2P3, Paris, France*
[o] *CEA, Irfu, SPP, Saclay, France*
[p] *IPHC, Université de Strasbourg, CNRS/IN2P3, Strasbourg, France*
[q] *IPNL, Université Lyon 1, CNRS/IN2P3, Villeurbanne, France*
[r] *Université de Lyon, Lyon, France*
[s] *III. Physikalisches Institut A, RWTH Aachen University, Aachen, Germany*
[t] *Physikalisches Institut, Universität Freiburg, Freiburg, Germany*
[u] *II. Physikalisches Institut, Georg-August-Universität Göttingen, Göttingen, Germany*
[v] *Institut für Physik, Universität Mainz, Mainz, Germany*
[w] *Ludwig-Maximilians-Universität München, München, Germany*
[x] *Fachbereich Physik, Bergische Universität Wuppertal, Wuppertal, Germany*
[y] *Panjab University, Chandigarh, India*
[z] *Delhi University, Delhi, India*
[aa] *Tata Institute of Fundamental Research, Mumbai, India*
[ab] *University College Dublin, Dublin, Ireland*
[ac] *Korea Detector Laboratory, Korea University, Seoul, Korea*
[ad] *CINVESTAV, Mexico City, Mexico*
[ae] *Nikhef, Science Park, Amsterdam, The Netherlands*
[af] *Radboud University Nijmegen, Nijmegen, The Netherlands*
[ag] *Joint Institute for Nuclear Research, Dubna, Russia*
[ah] *Institute for Theoretical and Experimental Physics, Moscow, Russia*
[ai] *Moscow State University, Moscow, Russia*
[aj] *Institute for High Energy Physics, Protvino, Russia*
[ak] *Petersburg Nuclear Physics Institute, St. Petersburg, Russia*
[al] *Institució Catalana de Recerca i Estudis Avançats (ICREA) and Institut de Física d'Altes Energies (IFAE), Barcelona, Spain*
[am] *Uppsala University, Uppsala, Sweden*
[an] *Lancaster University, Lancaster LA1 4YB, United Kingdom*
[ao] *Imperial College London, London SW7 2AZ, United Kingdom*
[ap] *The University of Manchester, Manchester M13 9PL, United Kingdom*
[aq] *University of Arizona, Tucson, AZ 85721, USA*
[ar] *University of California Riverside, Riverside, CA 92521, USA*
[as] *Florida State University, Tallahassee, FL 32306, USA*
[at] *Fermi National Accelerator Laboratory, Batavia, IL 60510, USA*
[au] *University of Illinois at Chicago, Chicago, IL 60607, USA*
[av] *Northern Illinois University, DeKalb, IL 60115, USA*
[aw] *Northwestern University, Evanston, IL 60208, USA*
[ax] *Indiana University, Bloomington, IN 47405, USA*
[ay] *Purdue University Calumet, Hammond, IN 46323, USA*
[az] *University of Notre Dame, Notre Dame, IN 46556, USA*
[ba] *Iowa State University, Ames, IA 50011, USA*
[bb] *University of Kansas, Lawrence, KS 66045, USA*

[bc] Kansas State University, Manhattan, KS 66506, USA
[bd] Louisiana Tech University, Ruston, LA 71272, USA
[be] Northeastern University, Boston, MA 02115, USA
[bf] University of Michigan, Ann Arbor, MI 48109, USA
[bg] Michigan State University, East Lansing, MI 48824, USA
[bh] University of Mississippi, University, MS 38677, USA
[bi] University of Nebraska, Lincoln, NE 68588, USA
[bj] Rutgers University, Piscataway, NJ 08855, USA
[bk] Princeton University, Princeton, NJ 08544, USA
[bl] State University of New York, Buffalo, NY 14260, USA
[bm] University of Rochester, Rochester, NY 14627, USA
[bn] State University of New York, Stony Brook, NY 11794, USA
[bo] Brookhaven National Laboratory, Upton, NY 11973, USA
[bp] Langston University, Langston, OK 73050, USA
[bq] University of Oklahoma, Norman, OK 73019, USA
[br] Oklahoma State University, Stillwater, OK 74078, USA
[bs] Brown University, Providence, RI 02912, USA
[bt] University of Texas, Arlington, TX 76019, USA
[bu] Southern Methodist University, Dallas, TX 75275, USA
[bv] Rice University, Houston, TX 77005, USA
[bw] University of Virginia, Charlottesville, VA 22904, USA
[bx] University of Washington, Seattle, WA 98195, USA

ARTICLE INFO

Article history:
Received 10 December 2012
Received in revised form 3 March 2013
Accepted 18 March 2013
Available online 21 March 2013
Editor: H. Weerts

ABSTRACT

We present the first combined measurement of the rapidity and transverse momentum dependence of dijet azimuthal decorrelations, using the recently proposed quantity $R_{\Delta\phi}$. The variable $R_{\Delta\phi}$ measures the fraction of the inclusive dijet events in which the azimuthal separation of the two jets with the highest transverse momenta is less than a specified value of the parameter $\Delta\phi_{\max}$. The quantity $R_{\Delta\phi}$ is measured in $p\bar{p}$ collisions at $\sqrt{s} = 1.96$ TeV, as a function of the dijet rapidity interval, the total scalar transverse momentum, and $\Delta\phi_{\max}$. The measurement uses an event sample corresponding to an integrated luminosity of 0.7 fb^{-1} collected with the D0 detector at the Fermilab Tevatron Collider. The results are compared to predictions of a perturbative QCD calculation at next-to-leading order in the strong coupling with corrections for non-perturbative effects. The theory predictions describe the data well, except in the kinematic region of large dijet rapidity intervals and small $\Delta\phi_{\max}$.

In high-energy collisions of hadrons, the production rates of particle jets with large transverse momentum with respect to the beam direction, p_T, are predicted by perturbative Quantum Chromodynamics (pQCD). At second order in the strong coupling constant, α_s, pQCD predicts only the production of dijet final states. In the absence of higher-order radiative effects, the jet directions are correlated in the azimuthal plane and their relative azimuthal angle $\Delta\phi_{\text{dijet}} = |\phi_{\text{jet1}} - \phi_{\text{jet2}}|$ is equal to π. Deviations from π (hereafter referred to as "azimuthal decorrelations") are caused by radiative processes in which additional jets are produced. The amount of the decorrelation is directly related to the jet multiplicity and to the p_T carried by the additional jets. The transition from soft to hard higher-order pQCD processes can be studied by examining the corresponding range of azimuthal decorrelations from small to large values. This makes measurements of dijet azimuthal decorrelations an ideal testing ground for pQCD predictions of multijet production processes. In pQCD, dijet azimuthal decorrelations are predicted to depend not only on the transverse momentum of the jets, but also on the dijet rapidity interval $y^* = |y_{\text{jet1}} - y_{\text{jet2}}|/2$, obtained from the rapidity difference of the two leading p_T jets in an event [1]. In a previous analysis of dijet azimuthal decorrelations in $p\bar{p}$ collisions at $\sqrt{s} = 1.96$ TeV, we measured the dijet differential cross section as a function of $\Delta\phi_{\text{dijet}}$, integrated over a fixed jet rapidity range and normalized by the inclusive dijet cross section for different requirements on the leading jet p_T [2]. The same methodology was later used in analyses of pp collision data at $\sqrt{s} = 7$ TeV from the CERN Large Hadron Collider [3,4]. In all cases, dijet azimuthal decorrelations have been observed to decrease with increasing p_T; however, the combined rapidity and p_T dependence has not yet been measured.

In this Letter, we perform a measurement of the rapidity and the p_T dependence of dijet azimuthal decorrelations in $p\bar{p}$ collisions at $\sqrt{s} = 1.96$ TeV, based on a data sample corresponding to an integrated luminosity of 0.7 fb^{-1} collected with the D0 detector at the Fermilab Tevatron Collider. The analysis is based on a new quantity, $R_{\Delta\phi}$, which was recently proposed in Ref. [5] as

$$R_{\Delta\phi}\left(H_T, y^*, \Delta\phi_{\max}\right) = \frac{\frac{d^2\sigma_{\text{dijet}}(\Delta\phi_{\text{dijet}} < \Delta\phi_{\max})}{dH_T\, dy^*}}{\frac{d^2\sigma_{\text{dijet}}(\text{inclusive})}{dH_T\, dy^*}}. \quad (1)$$

The quantity $R_{\Delta\phi}$ is defined as the fraction of the inclusive dijet cross section with a decorrelation of $\Delta\phi_{\text{dijet}} < \Delta\phi_{\max}$, where $\Delta\phi_{\max}$ is a parameter and $\sigma_{\text{dijet}}(\text{inclusive})$ is the inclusive dijet cross section without a $\Delta\phi_{\text{dijet}}$ requirement. It is measured as a function of $\Delta\phi_{\max}$, y^*, and the total transverse momentum H_T in the event, computed as the scalar p_T sum from all jets i with $p_{Ti} > p_{T\min}$ and $|y_i - y_{\text{boost}}| < y^*_{\max}$ where $y_{\text{boost}} = (y_{\text{jet1}} + y_{\text{jet2}})/2$, $y^*_{\max} = 2$, and $p_{T\min} = 30$ GeV, where jet1 and jet2 are the jets with the largest p_T in the event. For $\Delta\phi_{\max} \approx \pi$,

[1] Visitor from Augustana College, Sioux Falls, SD, USA.
[2] Visitor from The University of Liverpool, Liverpool, UK.
[3] Visitor from UPIITA–IPN, Mexico City, Mexico.
[4] Visitor from DESY, Hamburg, Germany.
[5] Visitor from SLAC, Menlo Park, CA, USA.
[6] Visitor from University College London, London, UK.
[7] Visitor from Centro de Investigacion en Computacion – IPN, Mexico City, Mexico.
[8] Visitor from ECFM, Universidad Autonoma de Sinaloa, Culiacán, Mexico.
[9] Visitor from Universidade Estadual Paulista, São Paulo, Brazil.

$R_{\Delta\phi}$ is sensitive to soft QCD radiation, while it becomes sensitive to hard higher-order QCD processes for smaller values of $\Delta\phi_{\max}$. Since $R_{\Delta\phi}$ is defined as a ratio of cross sections, several experimental and theoretical uncertainties cancel. In pQCD, for $2\pi/3 < \Delta\phi_{\max} < \pi$ ($\Delta\phi_{\max} \leqslant 2\pi/3$), the numerator of $R_{\Delta\phi}$ is a three-jet (four-jet) quantity [5]. Therefore, for $\Delta\phi_{\max} > 2\pi/3$, $R_{\Delta\phi}$ is computed as a ratio of three-jet and dijet cross sections which is (at leading order, LO) proportional to α_s. While dependencies on parton distribution functions (PDFs) largely cancel, $R_{\Delta\phi}$ is sensitive to the pQCD matrix elements and to α_s.

The measurement is performed for an inclusive dijet event sample defined by the Run II midpoint cone jet algorithm [6] with a cone of radius $R_{\text{cone}} = 0.7$ in y and ϕ. The dijet phase space is defined by the requirements $p_{T1} > H_T/3$, $p_{T2} > p_{T\min}$, $y^* < y^*_{\max}$, and $|y_{\text{boost}}| < 0.5$. Following the proposal in Ref. [5], $R_{\Delta\phi}$ is measured over the H_T range of 180–900 GeV, in three regions of the dijet rapidity interval of $0 < y^* < 0.5$, $0.5 < y^* < 1$, and $1 < y^* < 2$; and for $\Delta\phi_{\max} = 7\pi/8$, $5\pi/6$, and $3\pi/4$. The ranges in y^* and y_{boost}, and the value of $p_{T\min}$ ensure that all jets are always within $|y| < 2.5$ at p_T values where the jet energy calibration and jet p_T resolutions are known with high precision. The requirement $p_{T1} > H_T/3$ provides a lower boundary for the leading jet p_T in each H_T bin, which (together with $|y| < 2.5$) ensures that the jet triggers are efficient. The data are corrected for experimental effects and are presented at the "particle level," which includes all stable particles as defined in Ref. [7].

A detailed description of the D0 detector is provided in Ref. [8]. The event triggering and selection, jet reconstruction, and jet energy and momentum correction are identical to those used in recent D0 multijet measurements [9–13]. Jets are reconstructed in the finely segmented liquid-argon sampling calorimeters that cover most of the solid angle. The central calorimeter covers polar angles in the range 3–143° and the two endcap calorimeters extend this coverage to within 1.7° of the nominal beamline [8]. The transition regions between the central and the endcap calorimeters contain scintillator-based detectors to improve the energy sampling. The jet transverse momenta are calculated using only calorimeter information and the location of the $p\bar{p}$ collision. The position of the $p\bar{p}$ interaction is determined from the tracks reconstructed based on data from the silicon detector and scintillating fiber tracker located inside a 2 T solenoidal magnet [8]. The position is required to be within 50 cm of the detector center in the coordinate along the beam axis, with at least three tracks pointing to it. These requirements discard (7–9)% of the events, depending on the trigger used. For this measurement, events are triggered by inclusive jet triggers with prescales of 41.2 (for the lowest p_T trigger), 9.70, 1.39, and 1.0 (for the highest p_T trigger), respectively. Trigger efficiencies are studied as a function of H_T by comparing the inclusive dijet cross section in data sets obtained by triggers with different p_T thresholds in regions where the trigger with the lower threshold is fully efficient. The trigger with the lowest p_T threshold is shown to be fully efficient by studying an event sample obtained independently with a muon trigger. In each H_T bin, events are used from the trigger with the lowest prescale that has an efficiency higher than 98% in the corresponding H_T range. Requirements on the characteristics of the shower shapes of calorimeter clusters are used to suppress the background due to electrons, photons, and detector noise that would otherwise mimic jets. The signal efficiency for the shower shape requirements is above 97.5% [14,15]. Contributions from cosmic ray events are suppressed by requiring the missing transverse momentum in an event to be less than 70% (50%) of the leading jet p_T (before the jet energy calibration is applied) if the latter is below (above) 100 GeV. The efficiency of this requirement for signal is found to be $> 99.5\%$ [14,15]. After all selection requirements, the fraction of background events is below 0.1% for all H_T, as determined from distributions in signal and in background-enriched event samples.

The jet four-momenta reconstructed from calorimeter energy depositions are then corrected, on average, for the response of the calorimeter, the net energy flow through the jet cone, additional energy from previous beam crossings, and multiple $p\bar{p}$ interactions in the same event, but not for the presence of muons and neutrinos [14,15]. These corrections adjust the reconstructed jet energy to the energy of the stable particles that enter the calorimeter except for muons and neutrinos. The absolute energy calibration is determined from $Z \to e^+e^-$ events and the p_T imbalance in γ + jet events in the region $|y| < 0.4$. The extension to larger rapidities is derived from the p_T imbalance in dijet events with one jet at $|y| < 0.4$ and the other jet at larger $|y|$ [14,15]. In addition, corrections in the range (2–4)% are applied that take into account the difference in calorimeter response due to the difference in the fractional contributions of quark and gluon-initiated jets in the dijet and the γ + jet event samples. These corrections are determined using jets simulated with the PYTHIA event generator [16] that have been passed through a GEANT-based detector simulation [17]. The total corrections of the jet four-momenta vary between 50% and 20% for jet p_T between 50 and 400 GeV. An additional correction is applied for systematic shifts in rapidity due to detector effects [14,15].

The procedure that corrects the distributions $R_{\Delta\phi}(H_T, y^*, \Delta\phi_{\max})$ for experimental effects uses particle-level events, generated with SHERPA 1.1.3 [18] with MSTW2008LO PDFs [19] and with PYTHIA 6.419 [16] with CTEQ6.6 PDFs [20] and tune QW [21]. The jets from these events are processed by a simulation of the detector response which is based on parametrizations of jet p_T resolutions and jet reconstruction efficiencies determined from data and of resolutions of the polar and azimuthal angles of jets, obtained from a detailed simulation of the detector using GEANT.

The p_T resolution for jets is about 15% at 40 GeV, decreasing to less than 10% at 400 GeV. To use the simulation to correct for experimental effects, the simulation must describe all relevant distributions, including the p_T and $|y|$ distributions of the three leading p_T jets, and the $\Delta\phi_{\text{dijet}}$ distribution. To achieve this, the generated events, which are used in the correction procedure, are weighted, based on the properties of the generated jets, to match these distributions in data. The bin sizes in the H_T distributions are chosen to be approximately twice the H_T resolution. The bin purity, defined as the fraction of all reconstructed events that were generated in the same bin, is above 50% for all bins (and only weakly dependent on H_T), therefore it is sufficient to apply bin-by-bin correction factors to the data. We use the simulation to determine the correction factors for experimental effects for all bins. The correction factors are computed as the ratio of $R_{\Delta\phi}$ without and with simulation of the detector response. These also include corrections for the energies of unreconstructed muons and neutrinos inside the jets. The total correction factors for $R_{\Delta\phi}$ using the weighted PYTHIA and SHERPA simulations agree typically within 1% for $\Delta\phi_{\max} = 7\pi/8$ and $5\pi/6$ and between 1–4% for $\Delta\phi_{\max} = 3\pi/4$. The total correction factors, defined as the average values from PYTHIA and SHERPA, are 0.98–1.0 for $\Delta\phi_{\max} = 7\pi/8$, 0.95–0.99 for $\Delta\phi_{\max} = 5\pi/6$, and 0.81–0.91 for $\Delta\phi_{\max} = 3\pi/4$, with little y^* dependence. The difference between the average and the individual corrections is taken into account as the uncertainty attributed to the model dependence.

In total, 69 independent sources of experimental systematic uncertainties are identified, mostly related to jet energy calibration and jet p_T resolution. The effects of each source are taken as fully correlated between all data points. The dominant uncertainties for the $R_{\Delta\phi}$ distributions are due to the jet energy calibration (2–5)% and the model dependence of the correction factors (1–4)%.

Table 1
The results for $R_{\Delta\phi}$ with their relative uncertainties for $\Delta\phi_{\max} = 7\pi/8$.

H_T (GeV)	y^*	$R_{\Delta\phi}$	Stat. uncert. (percent)	Syst. uncert. (percent)	
180–205	0.0–0.5	2.216×10^{-1}	±0.9	+2.8	−3.0
205–235	0.0–0.5	2.116×10^{-1}	±1.1	+2.6	−2.6
235–270	0.0–0.5	2.000×10^{-1}	±1.5	+2.5	−2.3
270–310	0.0–0.5	1.811×10^{-1}	±2.2	+2.2	−2.2
310–360	0.0–0.5	1.731×10^{-1}	±1.5	+2.0	−2.1
360–415	0.0–0.5	1.641×10^{-1}	±2.4	+1.9	−1.9
415–470	0.0–0.5	1.491×10^{-1}	±1.5	+1.9	−1.9
470–530	0.0–0.5	1.359×10^{-1}	±2.4	+1.9	−1.9
530–600	0.0–0.5	1.206×10^{-1}	±3.2	+2.0	−2.0
600–680	0.0–0.5	1.204×10^{-1}	±5.0	+2.2	−2.1
680–770	0.0–0.5	1.114×10^{-1}	±8.8	+2.4	−2.3
770–900	0.0–0.5	9.699×10^{-2}	±15.4	+2.5	−2.3
180–205	0.5–1.0	2.311×10^{-1}	±0.9	+2.9	−3.3
205–235	0.5–1.0	2.252×10^{-1}	±1.2	+2.8	−2.9
235–270	0.5–1.0	2.115×10^{-1}	±1.6	+2.6	−2.5
270–310	0.5–1.0	2.085×10^{-1}	±2.3	+2.4	−2.3
310–360	0.5–1.0	1.888×10^{-1}	±1.7	+2.2	−2.2
360–415	0.5–1.0	1.808×10^{-1}	±2.8	+2.1	−2.1
415–470	0.5–1.0	1.686×10^{-1}	±1.8	+2.1	−2.0
470–530	0.5–1.0	1.662×10^{-1}	±2.8	+2.1	−2.1
530–600	0.5–1.0	1.517×10^{-1}	±3.9	+2.2	−2.1
600–680	0.5–1.0	1.318×10^{-1}	±7.3	+2.4	−2.1
680–770	0.5–1.0	1.356×10^{-1}	±13.0	+2.5	−2.2
180–205	1.0–2.0	2.934×10^{-1}	±1.0	+3.8	−4.4
205–235	1.0–2.0	2.850×10^{-1}	±1.3	+3.7	−4.0
235–270	1.0–2.0	2.634×10^{-1}	±2.0	+3.6	−3.4
270–310	1.0–2.0	2.667×10^{-1}	±2.9	+3.3	−2.9
310–360	1.0–2.0	2.502×10^{-1}	±2.3	+3.1	−2.6
360–415	1.0–2.0	2.468×10^{-1}	±4.0	+3.1	−2.6
415–470	1.0–2.0	2.317×10^{-1}	±3.0	+3.1	−2.7
470–530	1.0–2.0	2.320×10^{-1}	±5.2	+3.0	−2.7
530–600	1.0–2.0	2.116×10^{-1}	±8.6	+2.8	−2.8
600–680	1.0–2.0	2.875×10^{-1}	±13.7	+2.7	−2.8

Table 2
The results for $R_{\Delta\phi}$ with their relative uncertainties for $\Delta\phi_{\max} = 5\pi/6$.

H_T (GeV)	y^*	$R_{\Delta\phi}$	Stat. uncert. (percent)	Syst. uncert. (percent)	
180–205	0.0–0.5	1.439×10^{-1}	±1.1	+2.8	−2.6
205–235	0.0–0.5	1.325×10^{-1}	±1.4	+2.5	−2.5
235–270	0.0–0.5	1.223×10^{-1}	±2.0	+2.3	−2.3
270–310	0.0–0.5	1.097×10^{-1}	±3.0	+2.1	−2.1
310–360	0.0–0.5	1.007×10^{-1}	±2.1	+2.0	−2.0
360–415	0.0–0.5	9.851×10^{-2}	±3.3	+2.0	−1.9
415–470	0.0–0.5	8.635×10^{-2}	±2.1	+2.0	−2.0
470–530	0.0–0.5	7.821×10^{-2}	±3.2	+2.0	−2.0
530–600	0.0–0.5	6.832×10^{-2}	±4.3	+2.1	−2.1
600–680	0.0–0.5	7.262×10^{-2}	±6.6	+2.2	−2.3
680–770	0.0–0.5	5.760×10^{-2}	±12.5	+2.3	−2.4
770–900	0.0–0.5	5.600×10^{-2}	±20.7	+2.6	−2.7
180–205	0.5–1.0	1.463×10^{-1}	±1.4	+3.2	−2.9
205–235	0.5–1.0	1.396×10^{-1}	±1.6	+2.6	−2.6
235–270	0.5–1.0	1.317×10^{-1}	±2.2	+2.4	−2.5
270–310	0.5–1.0	1.263×10^{-1}	±3.1	+2.2	−2.3
310–360	0.5–1.0	1.139×10^{-1}	±2.3	+2.2	−2.2
360–415	0.5–1.0	1.117×10^{-1}	±3.6	+2.1	−2.1
415–470	0.5–1.0	1.016×10^{-1}	±2.4	+2.1	−2.1
470–530	0.5–1.0	9.993×10^{-2}	±3.8	+2.1	−2.1
530–600	0.5–1.0	9.414×10^{-2}	±5.1	+2.2	−2.2
600–680	0.5–1.0	8.566×10^{-2}	±9.2	+2.2	−2.3
680–770	0.5–1.0	7.369×10^{-2}	±18.2	+2.3	−2.5
180–205	1.0–2.0	1.926×10^{-1}	±1.3	+4.0	−3.5
205–235	1.0–2.0	1.840×10^{-1}	±1.8	+3.7	−3.5
235–270	1.0–2.0	1.709×10^{-1}	±2.6	+3.3	−3.4
270–310	1.0–2.0	1.716×10^{-1}	±3.9	+3.0	−3.2
310–360	1.0–2.0	1.611×10^{-1}	±3.0	+3.0	−3.1
360–415	1.0–2.0	1.600×10^{-1}	±5.2	+3.0	−3.1
415–470	1.0–2.0	1.436×10^{-1}	±4.0	+3.0	−3.0
470–530	1.0–2.0	1.518×10^{-1}	±6.7	+2.9	−3.1
530–600	1.0–2.0	1.391×10^{-1}	±11.0	+2.8	−3.1
600–680	1.0–2.0	2.034×10^{-1}	±17.2	+2.9	−3.2

Smaller contributions come from the jet ϕ resolution (0.5–2)%, from the uncertainties in systematic shifts in y ($< 2\%$), and the jet p_T resolution ($< 1\%$). All other sources are negligible. The systematic uncertainties are 2–3% for $\Delta\phi_{\max} = 7\pi/8$ and $5\pi/6$ and 3–5% for $\Delta\phi_{\max} = 3\pi/4$. A detailed documentation of the results, including the individual contributions to the uncertainties, is provided in the supplementary material [22].

The results for $R_{\Delta\phi}(H_T, y^*, \Delta\phi_{\max})$ are listed in Tables 1–3 and displayed in Fig. 1 as a function of H_T, in different regions of y^* and for different $\Delta\phi_{\max}$. A subset of the data points from selected H_T regions is also shown in Fig. 2, where $R_{\Delta\phi}$ is displayed as a function of y^* for different choices of $\Delta\phi_{\max}$. The values of H_T and y^* at which the data points are presented correspond to the arithmetic centers of the bins. Fig. 1 shows that for all choices of $\Delta\phi_{\max}$ and in all y^* regions, $R_{\Delta\phi}$ decreases with H_T. In all y^* regions, the H_T dependence increases towards lower $\Delta\phi_{\max}$, and for all $\Delta\phi_{\max}$ requirements the H_T dependence becomes stronger for smaller y^*. This implies that the y^* dependence of $R_{\Delta\phi}$ increases with increasing H_T, as shown in Fig. 2.

The theoretical predictions for $R_{\Delta\phi}$ are obtained from a pQCD calculation in next-to-leading order (NLO) in α_s with corrections for non-perturbative effects. The latter include contributions from hadronization and the underlying event. The non-perturbative corrections are determined using PYTHIA 6.426 with tunes AMBT1 [23] and DW [21], which use different parton shower and underlying event models. The hadronization correction is obtained from the ratio of $R_{\Delta\phi}$ on the parton level after the parton shower and the particle level including all stable particles, both without the underlying event. The underlying-event correction is computed from the ratio of $R_{\Delta\phi}$ computed at the particle level with and without underlying event. The total correction is given by the product of the two individual correction factors for hadronization and the underlying event. The total corrections vary between +1% and −1% for tune AMBT1 and between +1% and −3% for tune DW. The results obtained with the two tunes agree typically within 1% and always within 3% [5]. The central results are taken to be the average values, and the uncertainty is taken to be half of the difference. As a cross-check, the non-perturbative corrections are also derived with HERWIG 6.520 [24,25], using default settings. The HERWIG and PYTHIA results agree typically within 0.5%, and always within 1% (3%) for $\Delta\phi_{\max} = 7\pi/8$ and $5\pi/6$ (for $\Delta\phi_{\max} = 3\pi/4$) [5].

The NLO (LO) pQCD prediction for $R_{\Delta\phi}$ is computed as the ratio of the NLO (LO) predictions for the numerator and the denominator. The NLO prediction for the numerator (denominator) is obtained from an $\mathcal{O}(\alpha_s^4)$ ($\mathcal{O}(\alpha_s^3)$) cross section calculation. These results are computed using FASTNLO [26,27] based on NLOJET++ [28,29], in the $\overline{\text{MS}}$ scheme [30] for five active quark flavors. The calculations use the next-to-leading logarithmic (two-loop) approximation of the renormalization group equation and $\alpha_s(M_Z) = 0.118$ in the matrix elements and the PDFs, which is close to the current world average value of 0.1184 ± 0.0007 [31]. The MSTW2008NLO PDFs [19] are used, and the central choice μ_0 for the renormalization and factorization scales is $\mu_R = \mu_F = \mu_0 = H_T/2$, which is identical to $\mu_0 = p_T$ for inclusive jet and dijet production at LO. The theoretical predictions are overlaid on the data in Figs. 1 and 2, and some properties are displayed in Fig. 3. The PDF uncertainties are computed using the up and down variations of the 20 orthogonal PDF uncertainty eigenvectors, corresponding to the 68% C.L., as provided by MSTW2008NLO. The PDF uncertainties are typically 1%, and never larger than 2%. The $R_{\Delta\phi}$ results

Table 3
The results for $R_{\Delta\phi}$ with their relative uncertainties for $\Delta\phi_{\max} = 3\pi/4$.

H_T (GeV)	y^*	$R_{\Delta\phi}$	Stat. uncert. (percent)	Syst. uncert. (percent)	
180–205	0.0–0.5	4.659×10^{-2}	±2.0	+2.8	−2.7
205–235	0.0–0.5	4.339×10^{-2}	±2.6	+2.7	−2.5
235–270	0.0–0.5	4.055×10^{-2}	±3.5	+2.3	−2.2
270–310	0.0–0.5	3.405×10^{-2}	±5.4	+2.2	−2.2
310–360	0.0–0.5	2.913×10^{-2}	±4.0	+2.2	−2.2
360–415	0.0–0.5	2.733×10^{-2}	±6.2	+2.2	−2.3
415–470	0.0–0.5	2.419×10^{-2}	±4.0	+2.2	−2.4
470–530	0.0–0.5	2.008×10^{-2}	±6.3	+2.1	−2.6
530–600	0.0–0.5	1.780×10^{-2}	±8.4	+2.3	−2.8
600–680	0.0–0.5	1.953×10^{-2}	±12.6	+2.7	−3.1
680–770	0.0–0.5	2.241×10^{-2}	±19.8	+3.8	−3.5
180–205	0.5–1.0	4.620×10^{-2}	±2.6	+3.9	−3.9
205–235	0.5–1.0	4.261×10^{-2}	±3.0	+3.2	−3.1
235–270	0.5–1.0	4.152×10^{-2}	±3.9	+2.7	−2.7
270–310	0.5–1.0	3.510×10^{-2}	±6.0	+2.6	−2.8
310–360	0.5–1.0	3.578×10^{-2}	±4.1	+2.6	−2.9
360–415	0.5–1.0	2.962×10^{-2}	±7.1	+2.7	−2.9
415–470	0.5–1.0	3.107×10^{-2}	±4.3	+2.7	−2.9
470–530	0.5–1.0	2.984×10^{-2}	±6.9	+2.6	−2.9
530–600	0.5–1.0	2.532×10^{-2}	±9.8	+2.6	−3.2
600–680	0.5–1.0	2.587×10^{-2}	±16.7	+3.1	−3.4
180–205	1.0–2.0	6.873×10^{-2}	±2.5	+4.8	−3.9
205–235	1.0–2.0	6.402×10^{-2}	±3.3	+4.5	−4.1
235–270	1.0–2.0	6.169×10^{-2}	±4.6	+4.3	−4.5
270–310	1.0–2.0	6.741×10^{-2}	±6.4	+4.1	−4.8
310–360	1.0–2.0	5.218×10^{-2}	±5.5	+4.2	−4.7
360–415	1.0–2.0	5.049×10^{-2}	±9.5	+4.3	−4.5
415–470	1.0–2.0	4.505×10^{-2}	±7.2	+4.3	−4.4
470–530	1.0–2.0	4.899×10^{-2}	±11.9	+4.1	−4.7
530–600	1.0–2.0	3.504×10^{-2}	±22.0	+3.6	−5.6

obtained with the CT10 [32] and NNPDFv2.1 [33] PDF parametrizations agree with those for MSTW2008NLO within 2%. The theoretical uncertainties are dominated by the uncertainties of the pQCD calculations due to the μ_R and μ_F dependencies. These are computed as the relative changes of the results due to independent variations of both scales between $\mu_0/2$ and $2\mu_0$, with the restriction of $0.5 \leqslant \mu_R/\mu_F \leqslant 2.0$. The uncertainties from the scale dependence are 4–6% for $\Delta\phi_{\max} = 7\pi/8$ and $5\pi/6$, and 6–20% for $\Delta\phi_{\max} = 3\pi/4$, decreasing with H_T. In addition to the scale dependence, the NLO k-factors provide additional information on the convergence of the perturbative expansion, and therefore on the possible size of missing higher-order contributions. The NLO k-factors are computed as the ratio of the NLO and the LO predictions for $R_{\Delta\phi}$ ($k = R^{\mathrm{NLO}}_{\Delta\phi}/R^{\mathrm{LO}}_{\Delta\phi}$). Fig. 3 shows the inverse of the NLO k-factors and their dependence on y^* and $\Delta\phi_{\max}$.

Table 4
The χ^2 values between data and theory for MSTW2008PDFs and $\alpha_s(M_Z) = 0.118$ and for different choices of μ_R and μ_F. The results are shown for each of the nine kinematic regions, defined by the y^* and $\Delta\phi_{\max}$ requirements, combining all H_T bins inside those regions.

y^* range	$\Delta\phi_{\max}$	N_{dof}	χ^2 for $\mu_R = \mu_F =$		
			$H_T/4$	$H_T/2$	H_T
0.0–0.5	$7\pi/8$	12	15.1	7.1	12.7
0.0–0.5	$5\pi/6$	12	15.7	10.9	20.9
0.0–0.5	$3\pi/4$	11	13.1	44.2	104.5
0.5–1.0	$7\pi/8$	11	11.8	6.9	8.6
0.5–1.0	$5\pi/6$	11	5.6	4.0	12.6
0.5–1.0	$3\pi/4$	10	15.4	26.9	60.2
1.0–2.0	$7\pi/8$	10	29.7	24.4	19.8
1.0–2.0	$5\pi/6$	10	9.3	10.8	10.7
1.0–2.0	$3\pi/4$	9	10.3	23.1	45.5

Ratios of data and the theoretical predictions are displayed in Fig. 3 as a function of H_T in all regions of y^* and $\Delta\phi_{\max}$. To quantify the agreement, χ^2 values are determined that compare data and theory, taking into account the correlations between all uncertainties. The χ^2 definition is the same that was used in our recent α_s determinations [12,34]. Table 4 displays the χ^2 values for all H_T bins within each of the nine kinematic regions in y^* and $\Delta\phi_{\max}$. The results are shown for three different choices of μ_R and μ_F, including the central choice $\mu_R = \mu_F = H_T/2$ and the combined lower and upper variations, $H_T/4$ and H_T. The following discussion distinguishes between the three different kinematic regions, which are given by $\Delta\phi_{\max} = 3\pi/4$, by $y^* > 1$, and by $y^* < 1$ with $\Delta\phi_{\max} = 7\pi/8$ or $5\pi/6$.

The region of large azimuthal decorrelations, $\Delta\phi_{\max} = 3\pi/4$, is challenging for the theoretical predictions since it receives large contributions from four-jet final states. These are only modeled at LO by the $\mathcal{O}(\alpha_s^4)$ calculation for the numerator of $R_{\Delta\phi}$, which causes the large NLO k-factors (up to 1.5) and the large scale

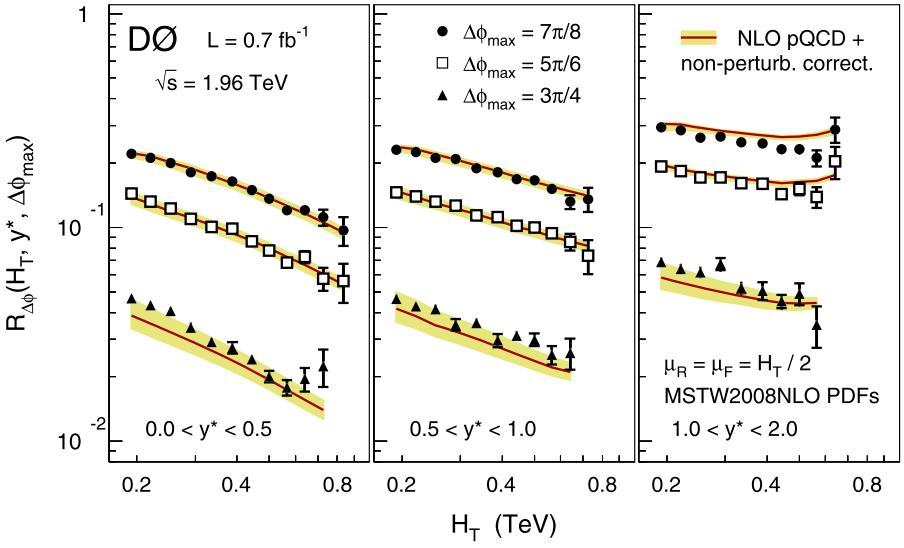

Fig. 1. (Color online.) The results for $R_{\Delta\phi}$ as a function of H_T in three different regions of y^* and for three different $\Delta\phi_{\max}$ requirements. The error bars indicate the statistical and systematic uncertainties summed in quadrature. The theoretical predictions are shown with their uncertainties.

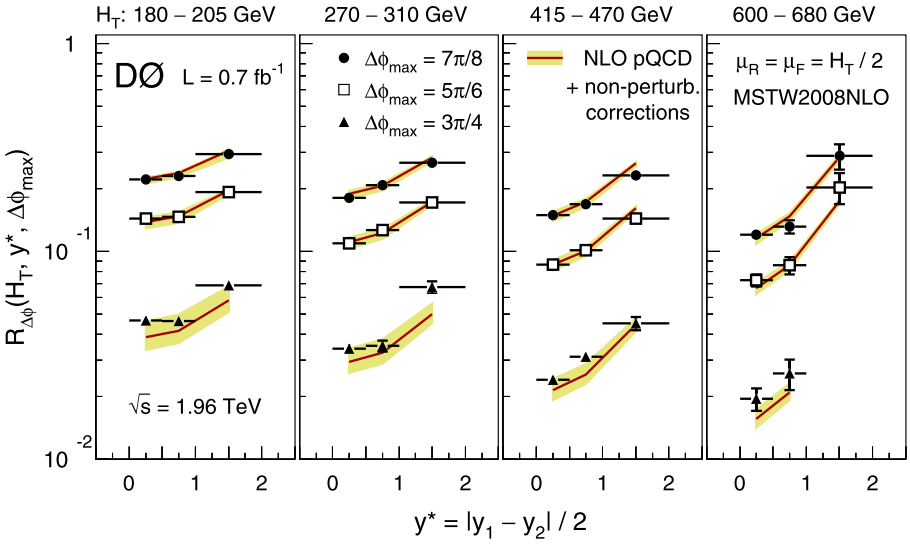

Fig. 2. (Color online.) The results for $R_{\Delta\phi}$ as a function of y^* in four different regions of H_T and for three different $\Delta\phi_{\max}$ requirements. The error bars indicate the statistical and systematic uncertainties summed in quadrature. The theoretical predictions are shown with their uncertainties.

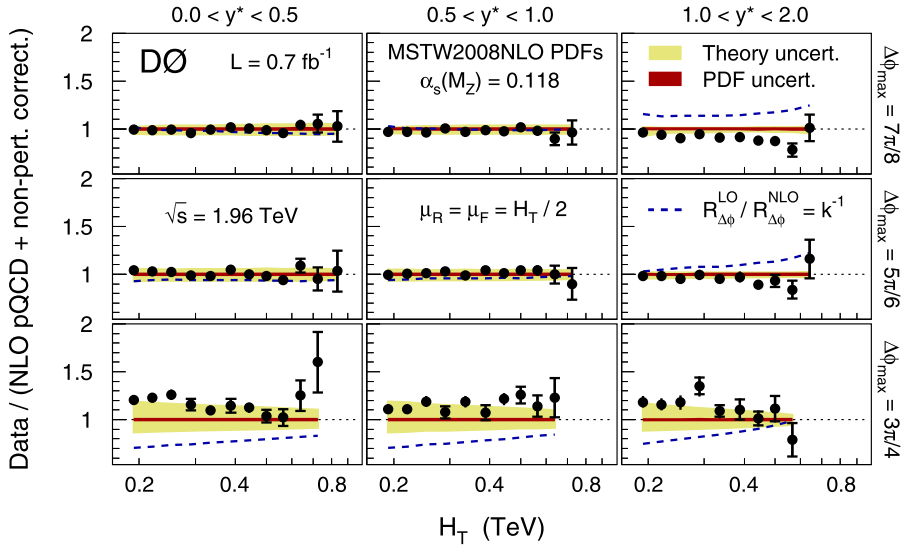

Fig. 3. (Color online.) Ratios of the results of $R_{\Delta\phi}$ and the theoretical predictions obtained for MSTW2008NLO PDFs and $\alpha_s(M_Z) = 0.118$. The ratios are shown as a function of H_T in different regions of y^* and for different $\Delta\phi_{\max}$. The inner error bars indicate the statistical uncertainties, and the outer error bars the statistical and systematic uncertainties summed in quadrature. The theoretical uncertainty is the PDF and scale uncertainty summed in quadrature. Also shown is the ratio of the LO and NLO pQCD predictions which is the inverse of the NLO k-factor.

dependence (up to 21%), seen in Fig. 3. In this kinematic region, the central theoretical predictions are consistently below the data (often by 15–25%). Within the large scale uncertainty, however, they agree with the data, as the χ^2 values for the lower scale choice $H_T/4$ are all consistent with the expectations based on the number of degrees of freedom (N_{dof}, which corresponds here to the number of data points), of $\chi^2 = N_{\text{dof}} \pm \sqrt{2N_{\text{dof}}}$.

In the kinematic region $y^* > 1$, the theoretical predictions exhibit a different H_T dependence as compared to lower y^*, as seen in Fig. 1. While at lower y^* the predicted H_T dependence of the $R_{\Delta\phi}$ distributions is monotonically decreasing, the H_T distributions for $y^* > 1$ have a local minimum around ≈ 0.5 TeV above which $R_{\Delta\phi}$ increases. For $\Delta\phi_{\max} = 5\pi/6$, the theoretical predictions give an adequate description of the data. For $\Delta\phi_{\max} = 7\pi/8$, however, the predicted H_T dependence differs from that of the measured $R_{\Delta\phi}$ distribution, as quantified by the large χ^2 regardless of the scale choice. This is the only kinematic region in ($\Delta\phi_{\max}$, y^*) for which the NLO k-factor is consistently below unity (0.89–0.81) over the entire H_T range. This may indicate a poor convergence of the perturbative expansion.

The perturbative expansion works best in the kinematic regions of $0 < y^* < 0.5$ and $0.5 < y^* < 1.0$, where the scale dependence is small ($< 6\%$) and the NLO k-factors are above unity but small ($1.00 < k < 1.06$). In all of those regions, the theoretical predictions give a good description of the data.

In summary, the first measurement of the combined rapidity and p_T dependence of dijet azimuthal decorrelations is presented. The measurement is based on the recently proposed quantity $R_{\Delta\phi}$, which probes dijet azimuthal decorrelations in a novel way. It is measured in $p\bar{p}$ collisions at $\sqrt{s} = 1.96$ TeV as a function of the total transverse momentum H_T, the dijet rapidity interval y^*, and the parameter $\Delta\phi_{\max}$. For all values of $\Delta\phi_{\max}$ and at fixed H_T, dijet azimuthal decorrelations increase with y^*, while they decrease with H_T over most of the H_T range at fixed y^*. Predictions of

NLO pQCD, corrected for non-perturbative effects, give a good description of the data, except in the kinematic region of large dijet rapidity intervals $y^* > 1$ and small decorrelations $\Delta\phi_{\max} = 7\pi/8$.

Acknowledgements

We thank the staffs at Fermilab and collaborating institutions, and acknowledge support from the DOE and NSF (USA); CEA and CNRS/IN2P3 (France); MON, NRC KI and RFBR (Russia); CNPq, FAPERJ, FAPESP and FUNDUNESP (Brazil); DAE and DST (India); Colciencias (Colombia); CONACyT (Mexico); NRF (Korea); FOM (The Netherlands); STFC and the Royal Society (United Kingdom); MSMT and GACR (Czech Republic); BMBF and DFG (Germany); SFI (Ireland); The Swedish Research Council (Sweden); and CAS and CNSF (China).

Appendix A. Supplementary material

Supplementary material related to this article can be found online at http://dx.doi.org/10.1016/j.physletb.2013.03.029.

References

[1] Rapidity y is related to the polar scattering angle θ with respect to the proton beam direction by $y = \frac{1}{2}\ln[(1+\beta\cos\theta)/(1-\beta\cos\theta)]$, where β is defined as the ratio of the magnitude of momentum and energy, $\beta = |\vec{p}|/E$. In $2 \to 2$ processes, the variable y^* corresponds to the absolute value of the rapidities of the two jets in the dijet center-of-mass frame (see Ref. [5]).
[2] V.M. Abazov, et al., D0 Collaboration, Phys. Rev. Lett. 94 (2005) 221801.
[3] V. Khachatryan, et al., CMS Collaboration, Phys. Rev. Lett. 106 (2011) 122003.
[4] G. Aad, et al., ATLAS Collaboration, Phys. Rev. Lett. 106 (2011) 172002.
[5] M. Wobisch, et al., J. High Energy Phys. 1301 (2013) 172.
[6] G.C. Blazey, et al., in: U. Baur, R.K. Ellis, D. Zeppenfeld (Eds.), Proceedings of the Workshop: QCD and Weak Boson Physics in Run II, Fermilab-Pub-00/297, 2000.
[7] C. Buttar, et al., in: G. Belanger, et al. (Eds.), Les Houches 2007, Physics at TeV Colliders, arXiv:0803.0678 [hep-ph], Section 9.
[8] V.M. Abazov, et al., D0 Collaboration, Nucl. Instrum. Methods Phys. Res. A 565 (2006) 463.
[9] V.M. Abazov, et al., D0 Collaboration, Phys. Rev. Lett. 103 (2009) 191803.
[10] V.M. Abazov, et al., D0 Collaboration, Phys. Lett. B 693 (2010) 531.
[11] V.M. Abazov, et al., D0 Collaboration, Phys. Lett. B 704 (2011) 434.
[12] V.M. Abazov, et al., D0 Collaboration, Phys. Lett. B 718 (2012) 56.
[13] V.M. Abazov, et al., D0 Collaboration, Phys. Lett. B 720 (2013) 6.
[14] V.M. Abazov, et al., D0 Collaboration, Phys. Rev. Lett. 101 (2008) 062001.
[15] V.M. Abazov, et al., D0 Collaboration, Phys. Rev. D 85 (2012) 052006.
[16] T. Sjöstrand, et al., Comput. Phys. Commun. 135 (2001) 238.
[17] R. Brun, F. Carminati, CERN Program Library Long Writeup W5013, 1993.
[18] T. Gleisberg, et al., J. High Energy Phys. 0902 (2009) 007.
[19] A.D. Martin, et al., Eur. Phys. J. C 63 (2009) 189.
[20] P.M. Nadolsky, et al., Phys. Rev. D 78 (2008) 013004.
[21] M.G. Albrow, et al., TeV4LHC QCD Working Group, hep-ph/0610012.
[22] Supplementary material is available in the online version of this Letter at http://dx.doi.org/10.1016/j.physletb.2013.03.029.
[23] G. Brandt, in: M. Diehl, J. Haller, T. Schörner-Sadenius, G. Steinbrück (Eds.), 5th Conference: Physics at the LHC 2010, DESY-PROC-2010-01, 2010.
[24] G. Corcella, et al., J. High Energy Phys. 0101 (2001) 010.
[25] G. Corcella, et al., hep-ph/0210213.
[26] T. Kluge, K. Rabbertz, M. Wobisch, hep-ph/0609285.
[27] M. Wobisch, et al., fastNLO Collaboration, arXiv:1109.1310 [hep-ph].
[28] Z. Nagy, Phys. Rev. D 68 (2003) 094002.
[29] Z. Nagy, Phys. Rev. Lett. 88 (2002) 122003.
[30] W.A. Bardeen, A.J. Buras, D.W. Duke, T. Muta, Phys. Rev. D 18 (1978) 3998.
[31] J. Beringer, et al., Particle Data Group, Phys. Rev. D 86 (2012) 010001.
[32] H.L. Lai, et al., Phys. Rev. D 82 (2010) 074024.
[33] R.D. Ball, et al., Nucl. Phys. B 849 (2011) 296.
[34] V.M. Abazov, et al., D0 Collaboration, Phys. Rev. D 80 (2009) 111107.